NeuroImage: Clinical 44 (2024) 103706

Contents lists available at ScienceDirect

NeuroImage: Clinical

journal homepage: www.elsevier.com/locate/ynicl

Blood-brain barrier disruption and increased free water are associated with worse cognitive performance in patients with chronic cerebrovascular disease

Kyle C. Kern [a,b], Marwah S. Zagzoug [a], Rebecca F. Gottesman [a], Clinton B. Wright [a], Richard Leigh [a,c,*]

[a] National Institute of Neurological Disorders and Stroke, National Institutes of Health, Bethesda, MD, United States
[b] Department of Neurology, University of California Los Angeles David Geffen School of Medicine, Los Angeles, CA, United States
[c] Department of Neurology, Johns Hopkins University School of Medicine, Baltimore, MD, United States

ARTICLE INFO

Keywords:
Magnetic resonance imaging
Blood-brain barrier
Diffusion tensor imaging
Free water
Dementia
Vascular
White Matter Hyperintensities
Cerebral Small Vessel Diseases
Ischemic Stroke

ABSTRACT

Progression of cerebral small vessel disease (CSVD) is associated with cognitive decline. Blood-brain barrier disruption (BBBD) and fluid extravasation to the interstitial space may contribute to progression of white matter hyperintensities (WMH). We hypothesized that increased free water (FW) would colocalize with BBBD and relate to cognitive performance. Patients with ischemic stroke/TIA at least 3 months prior with at least early confluent WMH were studied cross-sectionally with the Montreal Cognitive Assessment (MoCA), diffusion tensor imaging, and dynamic susceptibility contrast imaging. White matter (WM) was segmented into WMH, WMH penumbra, and normal appearing white matter (NAWM). Colocalization of elevated FW and BBBD and their associations with MoCA performance were evaluated. 58 patients were included (mean age 69, 36 % female). Higher BBBD colocalized with elevated FW. Elevated FW in all white matter, NAWM, WMH penumbra, and WMH lesions was associated with lower MoCA score. Increased BBBD in all WM, NAWM, and WMH penumbra was associated with lower MoCA. In WMH penumbra, both elevated FW and increased BBBD were independently associated with lower MoCA. We found agreement between 2 different biomarkers implicated in the pathogenesis of CSVD that independently demonstrated association with cognitive performance when measured in the area of postulated disease activity.

1. Background

The vascular contributions to cognitive impairment and dementia (VCID) are largely driven by progressive cerebral small vessel disease (CSVD) due to aging and vascular risk factors. The most well-recognized biomarker for CSVD is increased T2 signal in the white matter on MRI, or white matter hyperintensities (WMH) (Fazekas et al., 2013). As the burden of WMH increases, so does the risk of VCID (Debette and Markus, 2010), and when normal appearing white matter (NAWM) progresses into WMH, the risk of VCID is even higher (Kloppenborg et al., 2014). With subclinical infarction, or after suffering a symptomatic stroke, the risk of developing VCID is higher still (Savva and Stephan, 2010). The progression of CSVD may also be a driver of post-stroke cognitive impairment.

Another biomarker for CSVD is the loss of white matter microstructure detected with diffusion tensor imaging (DTI). Conventional DTI can detect CSVD progression as reduced fractional anisotropy (FA) and increased mean diffusivity (MD), both indicating reduced white matter integrity. However, these changes are not limited to the WMH, and often involve adjacent areas of NAWM, which is the region at greatest risk for progression to WMH and is often referred to as the WMH penumbra (Maillard et al., 2011). Since changes in MD and FA precede the development of WMH, they likely reflect early pathogenesis of WMH. This loss of microstructure has been attributed to myelin disruption due to a hypoxic and proinflammatory environment (Rosenberg et al., 2016). It is thought that blood-derived proteins cross a disrupted blood–brain barrier (BBB), leading to degradation of white matter. DTI-derived free water (FW) is also increased in the WMH penumbra (Mayer et al., 2022; Kern et al., 2023). Since water freely diffuses back and forth across the BBB, the accumulation of FW into the

* Corresponding author at: 600 N. Wolfe Street, Phipps 4, Suite 446, Baltimore, MD 21287, United States
E-mail address: rleigh4@jhu.edu (R. Leigh).

https://doi.org/10.1016/j.nicl.2024.103706
Received 26 June 2024; Received in revised form 19 October 2024; Accepted 10 November 2024
Available online 13 November 2024
2213-1582/© 2024 The Author(s). Published by Elsevier Inc. This is an open access article under the CC BY-NC-ND license (http://creativecommons.org/licenses/by-nc-nd/4.0/).

brain parenchyma is presumably due to water following osmolar gradients from proinflammatory molecules that have traversed a disrupted BBB, though mechanisms of water transport, including trafficking of aquaporin 4 molecules in response to injury and osmotic changes, are poorly understood.

Given this proposed mechanism for the pathogenesis of WMH, we hypothesized that in participants with CSVD and a prior history of stroke, measurements of FW would be increased in areas where BBB disruption (BBBD) was detected. Since FW and BBBD may be complementary biomarkers for VCID and post-stroke cognitive impairment, we also tested whether each biomarker related to cognitive performance.

2. Methods

2.1. Human Research Protocol

The Deputy Ethics Counselors and Institutional Review Boards of NINDS/NIH (IRB Protocol Number: 18 N0020), Suburban Hospital, Johns Hopkins Medicine, Bethesda, MD (Protocol Number: IRB00156306), and MedStar Washington Hospital Center, Washington, DC (Protocol Number: 2018–093) approved this study, and it is registered with clinicaltrials.gov (NCT03366129). All subjects provided written informed consent.

2.2. Data Integrity and Availability

The corresponding author oversaw the integrity of data collection and analysis. Results are presented according to STROBE criteria for observational studies. Upon reasonable request to the corresponding author, the data will be made available after close-out and publication of the parent study under a formal data sharing agreement and with approval from the requesting researcher's local ethics committee. The software used in the study is freely available for non-commercial use (Freesurfer, FSL, DIPY) or commercially available (Matlab, Stata).

2.3. Study Population

This is a cross-sectional analysis of subjects enrolled in a longitudinal study in which participants were eligible if they had a history of stroke or TIA and demonstrated CSVD on their MRI scan in the form of at least early confluent WMH (Fazekas grade 2). Participants were excluded if they were unable to ambulate independently, could not communicate verbally in English, had concurrent neurologic disease predisposing them to WMH of non-cerebrovascular origin, or had severe dementia based on cognitive screening. Participants were excluded if they had a Montreal Cognitive Assessment (MoCA) score less than 14, or a six-item screener score less than 4. Enrolled participants had an MRI scan performed at least 3 months after their clinical stroke or TIA. Cognitive testing with the MoCA was performed on the same day as the MRI scan. Education was self-reported and categorized as high-school or G.E.D., some college or associate degree, bachelor degree, or graduate or professional degree since none reported less than high-school education. Race and ethnicity were self-reported. Race was included in statistical analysis as Black vs. all other.

2.4. MRI Protocol

MRI scans were performed at two hospital sites using either a 3 T Siemens Skyra or a 3 T Phillips Achieva. The acquisition included a 3D T1 (resolution 1x1x1mm), a 3D FLAIR (resolution 1x1x1mm), an axial FLAIR (resolution ~ 1x1x3.5 mm), DTI (Siemens: 12 directional images with B = 1000 s/mm^2, 4B = 0 images, and resolution 1.7x1.7x3.5 mm or Phillips: 15 directions at B = 1000 s/mm^2, 1B = 0 image, and 2x2x3.5 mm), and dynamic susceptibility contrast (DSC) perfusion weighted imaging (PWI) (Siemens: 80 volumes, TE: 25 ms, TR: 1.2 s, flip angle: 80 degrees, resolution: 2.3x2.3x7mm; Philips: 120 Volumes, TE: 25 ms, TR 1 s, flip angle 75 degrees, resolution: 1.9x1.9x7mm), which was collected during a single injection of a weight-based dose of gadolinium (0.1 mmol/kg) using either Gadavist (gadobutrol, Bayer Schering Pharma, Whippany, New Jersey) or Multihance (gadobenate dimeglumine, Bracco Diagnostics, Monroe Township, New Jersey) at a flow rate of 5 mL/sec.

2.5. MRI Processing

DTI data were corrected for head motion and eddy current distortions using FSL's Eddy, and a tensor was fit at each voxel using linear regression, from which conventional fractional anisotropy and mean diffusivity were calculated. Next, DTI free water fraction was calculated at each voxel by fitting a regularized two-compartment model to the diffusion signal using DIPY (Golub et al., 2021). The free water fraction reflects the fraction of the diffusion signal attributable to a CSF-like, isotropic tensor with the diffusivity of water at 37 degrees ($3x10^{-3}$ mm^2/s). The remaining, FW-corrected diffusion signal comprised the modelled tissue compartment, from which we calculated a tensor as well as FW-corrected diffusion metrics: FW-corrected mean diffusivity (MDc) and FW-corrected fractional anisotropy (FAc).

DSC source images were processed independent of the DTI analysis to detect and quantify leakage of contrast through the BBB (Leigh et al., 2012). After correction for head motion, the DSC time-dependent signal at each voxel was modelled as a combination of intravascular and extravascular components. In the absence of BBBD, the passage of a bolus through the cerebral vasculature causes hypointensity due to T2* susceptibility. However, in the setting of BBBD, gadolinium leakage into the brain parenchyma causes relative hyperintensity due to a T1 effect that is proportional to the concentration of gadolinium in the tissue (Zaharchuk, 2007). Thus, in the setting of BBBD, the area under the gadolinium concentration curve is decreased proportionally to the amount of BBB leakage (Boxerman et al., 2006). By modeling the recorded signal as a sum of the intravascular and extravascular components, and accounting for regional differences in blood flow, the signal due to BBBD can be isolated (Leigh et al., 2012). BBBD is quantified as the percent of the recorded signal that has been lost due to contrast leakage through the BBB. This approach to measuring BBBD has been used by other groups to study white matter injury in stroke patients (Rost et al., 2018). The method described here has been replicated and validated in animals (Jin et al., 2019) and independently implemented on a 3rd party software platform to study stroke-related BBBD (Bani-Sadr et al., 2023). However, for the current study, in-house software developed in Matlab was used.

For each participant, the fourth DSC volume was aligned to the DTI B0 image, and the transformation was subsequently applied to the entire 4D DSC dataset. Conventional FA images were nonlinearly aligned to the MNI FA atlas, and the reverse transform was calculated to project an atlas-derived white matter region-of-interest (ROI) mask into each participant's native DTI space.

In parallel, the FLAIR and T1 images were used to segment WMH using Freesurfer's Samseg (Cerri et al., 2021). These WMH masks were visually checked and manually edited as needed for accuracy. FLAIR hyperintensity due to chronic infarct could not be reliably distinguished from background WMH and so was included in the WMH ROI. WMH masks were aligned into native DTI space using a T1 to FA alignment. The penumbra was defined as the NAWM surrounding the WMH and was isolated by dilating the WMH lesions by 3 mm and then subtracting the non-dilated lesions (Fig. 1A and B). The NAWM mask was used to limit the penumbra and exclude any dilation into gray matter or CSF. A 3 mm penumbra was used since new WMH progression is most likely to occur in this region (Promjunyakul et al., 2015). The resulting ROIs used in the study were all WM, NAWM, penumbra, and WMH, from which mean BBBD and mean FW were derived. The WMH volume fraction was calculated relative to the total intracranial volume.

To compare BBBD (which is expressed as the percentage of signal loss

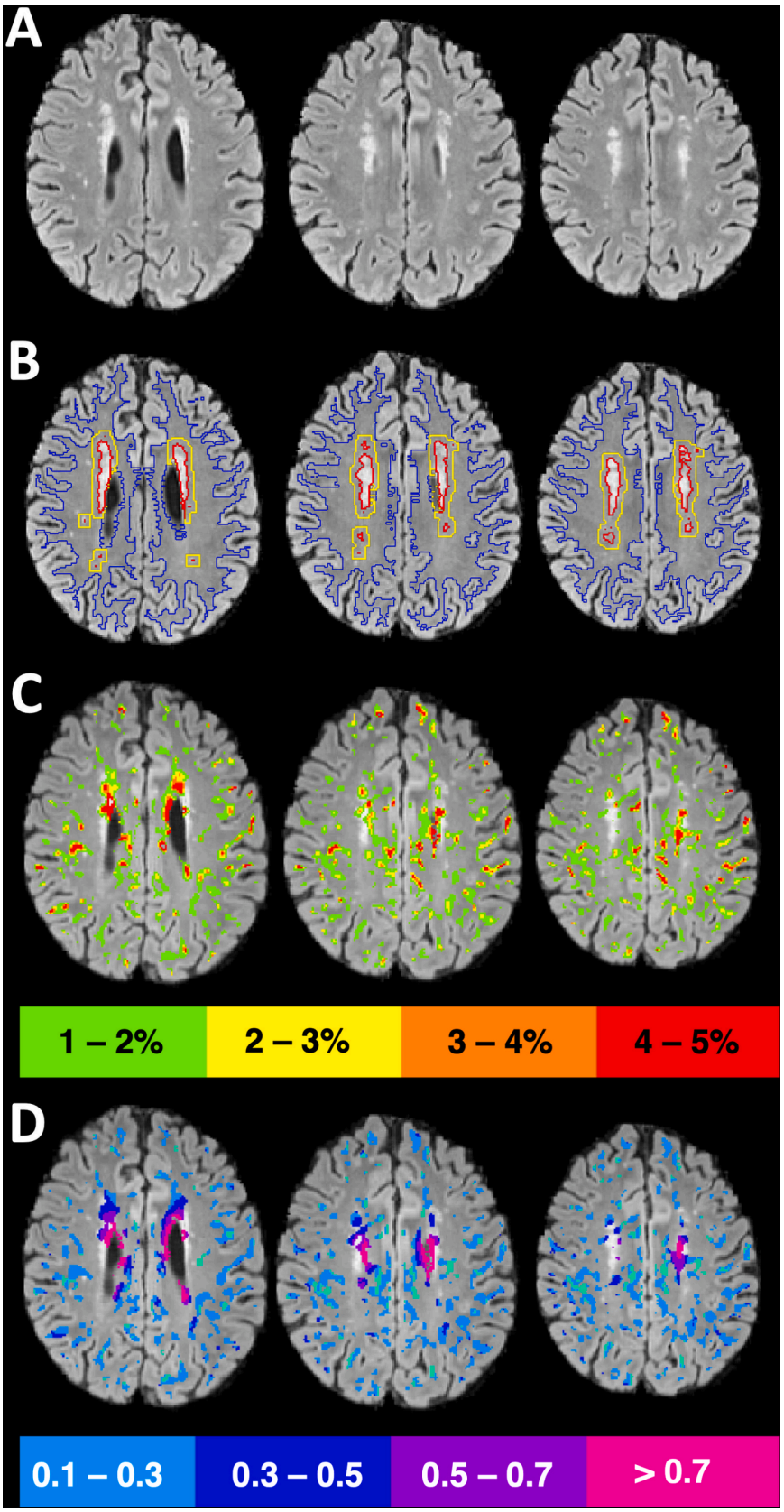

Fig. 1. Methods. A) FLAIR axial slices show white matter hyperintensities (WMH) in the periventricular area and the corona radiata. B) Tissue was segmented into WMH (red), WMH penumbra (yellow), and normal appearing white matter (blue). C) Regions of relative blood–brain barrier disruption (BBBD) across all white matter were divided into echelons (only 4 pictured here for clarity) and overlaid on the FLAIR image. D) Within each echelon of BBBD, the mean free water (FW) was calculated, colorized, and overlaid on the FLAIR image. In regions of increased BBBD, mean FW was higher, demonstrating colocalization between these two biomarkers. (For interpretation of the references to color in this figure legend, the reader is referred to the web version of this article.)

due to leakage through the BBB) with FW, the voxels within white matter from the BBB images were divided into 10 bins, or echelons, each covering a half a percentage range and increasing from zero to 5 % (i.e. < 0.5 %, 0.5–1 % … 4–4.5 %, 4.5–5 %). To compare the severity of BBBD to colocalized FW accumulation, we calculated the mean FW within voxels contributing to each BBB echelon (Fig. 1C and D). BBBD measurements were calculated by one author (R.L.) who was blinded to the results of the DTI analysis; FW measurements were calculated by one author (K.C.K.) who was blinded to the results of the BBBD analysis.

2.6. Statistical Analysis

Mixed-effects linear regression (MELR) was used to account for repeated measures and test for differences across white matter regions (NAWM, Penumbra, or WMH) for FW or BBBD (separately). The MELR models included participant and MRI site as random effects, and fixed effects for white matter region, age, sex, and race. To account for multiple pairwise comparisons of regions, a Bonferroni correction was applied.

To test for colocalization of BBBD and FW, for each participant ten BBBD echelons across all WM were used to predict the mean FW within each region circumscribed by a BBBD echelon. MELR was used to estimate across all participants the association between BBBD echelon and colocalized mean FW. Random effects included intercept for each participant and MRI site, while fixed effects included a quadratic term for BBBD echelon, age, sex, and race. A quadratic term for BBBD was used after visualizing the spaghetti plot, and a likelihood ratio test was used to confirm better fit of the quadratic term compared to the linear term.

Separate MELR were used to determine the associations between BBBD and each DTI metric: FW, FAc and MDc. DTI metrics were standardized to a Z-score using the mean and standard deviation across all participants. To compare the relative strengths of the associations across DTI metrics, we compared the standardized coefficients and the R^2 values for each MELR model. Each model included random effects for participant intercept and fixed effects for the covariates age, sex, race, and MRI site.

Finally, to test the associations between imaging markers and cognitive performance, we first used unadjusted regression to predict MoCA score with either FW or BBBD across all WM, and subsequently across each WM subregion: WMH, penumbra, and NAWM. Based on these results, we tested an adjusted MELR model to predict MoCA that included fixed effects for mean BBBD and mean FW within the penumbra, age, sex, race, and education, and a random effect for MRI site. For each model, we evaluated for normality of the residuals, heteroscedasticity, and collinearity to ensure the assumptions of linear regression were met.

3. Results

3.1. Participant and Imaging Characteristics

There were 58 participants included in the study. The median age (± SD) was 69 ± 9 years and 36 % were female. The median WMH volume at the time of study participation was 13.9 mL (IQR = 13.7), and mean MoCA score (± SD) was 26 ± 3. The study visit occurred at a median of 203 days (IQR = 102) after the index ischemic event. Table 1 summarizes the participant characteristics.

3.2. Characteristics of the Index Ischemic Event

Medical records and prior brain imaging for the index ischemic event were reviewed for each enrolled participant. The index ischemic event was stroke in 55 (95 %), central retinal artery occlusion in 1, and transient ischemic attack (TIA) in 2. Of the participants with TIA, one had a chronic lacune at TIA presentation, while the other presented with a transient territorial perfusion delay that localized with presenting neurologic symptoms. Of those with acute infarct confirmed on diffusion imaging at the time of the index event, 28 (48 %) had a cortical infarct, 24 (41 %) had a subcortical infarct, and 6 (10 %) had a cerebellar infarct. Index stroke etiology by TOAST criteria (Adams et al., 1993) was determined to be small vessel occlusion (SVO) in 16 (28 %), large artery atherosclerosis (LAA) in 10 (17 %), cardioembolic (CE) in 15 (26 %), and cryptogenic in 15 (26 %). Of cryptogenic strokes, 14 were embolic strokes of unknown source (ESUS).

Table 1
Participant Characteristics (N = 58).

Mean Age (SD) years	70 (9)
# Female	21 (36 %)
Race	
White	37 (64 %)
Black	16 (28 %)
Asian	3 (5 %)
Ethnicity	
Hispanic or Latino	4 (7 %)
Education	
High School or G.E.D	10 (17 %)
Some College or Associate's Degree	7 (12 %)
Bachelor's Degree	12 (21 %)
Graduate or Professional Degree	29 (50 %)
Vascular Risk Factors	
Hypertension	47 (81 %)
Hyperlipidemia	31 (53 %)
Diabetes Mellitus Type 2	22 (38 %)
Atrial Fibrillation	17 (29 %)
Obstructive Sleep Apnea	10 (17 %)
Coronary Artery Disease	8 (14 %)
Cardiomyopathy	5 (9 %)
Index Ischemic Event	
Stroke	55 (95 %)
Central Retinal Artery Occlusion	1 (2 %)
Transient Ischemic Attack	2 (3 %)
Median Days Since Event (IQR)	203 (102)
Index Stroke Location	
Cortical	28 (48 %)
Subcortical	24 (41 %)
Cerebellar	6 (10 %)
Index Event TOAST Criteria	
Small Vessel Occlusion	16 (28 %)
Large Artery Atherosclerosis (8 ICAD, 2 ECAD)	10 (17 %)
Cardioembolic (10 Afib, 1 CMY, 1 myxoma)	12 (21 %)
Cryptogenic (14 ESUS)	15 (26 %)
Other Known Cause (1 Dissection, 1 periprocedural)	2 (3 %)
Baseline Imaging Findings	
Median WMH Volume mL (IQR)	13.9 (13.7)
Mean Brain Parenchymal Fraction (SD)	68.5 % (3.7)
Presence of Lacunes	27 (47 %)
Presence of Cortical Infarcts	23 (40 %)
Presence of Cerebral Microbleeds	18 (31 %)

Afib = atrial fibrillation; CMY = cardiomyopathy; ECAD = extracranial atherosclerotic disease; ESUS = embolic stroke of unknown source; ICAD = intracranial atherosclerotic disease; SD = standard deviation; IQR = interquartile range; TOAST = Trial of ORG 10172 in Acute Stroke Treatment (Adams et al., 1993); WMH = white matter hyperintensity.

3.3. Free Water and Blood-Brain Barrier Disruption across White Matter Regions

Mean FW was highest in the WMH lesions (0.49 ± 0.07), intermediate in the penumbra (0.29 ± 0.04), and lowest in the NAWM (0.20 ± 0.03; $p < 0.001$ for all pairwise comparisons; Fig. 2A). Mean BBBD was also highest in the WMH (0.011 % ± 0.0069 %), greater than within the penumbra (0.0086 % ± 0.0038 %) or NAWM (0.0091 % ± 0.0038 %; $p < 0.001$, Fig. 2B). Mean BBBD in the penumbra was not significantly different than in the NAWM ($p = 1$).

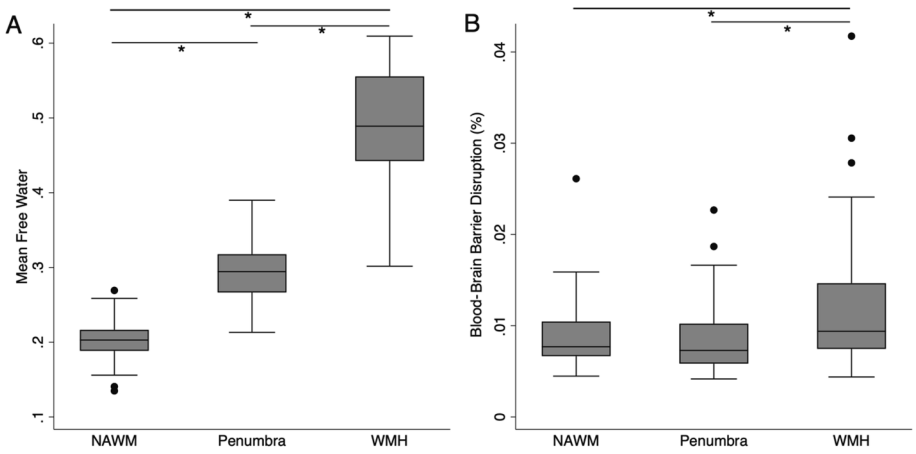

Fig. 2. White matter pathology relates to free water and blood–brain barrier disruption. White matter was segmented into white matter hyperintensities (WMH), a WMH penumbra after dilating by 3 mm, and normal appearing white matter (NAWM). A) Mean free water (FW) was different across each white matter region. B) Mean blood-brain barrier disruption (BBBD) was elevated in WMH relative to penumbra or NAWM. There was no difference between mean BBBD in NAWM and penumbra. *Indicates pairwise comparison with $p < 0.001$.

3.4. Elevated Free Water Colocalizes with Blood-Brain Barrier Disruption

For each participant, all white matter was divided into ten echelons reflecting the severity of BBBD (range 0 to 5 %, interval 0.5 %). The mean FW within each echelon was plotted for each participant as a spaghetti plot, demonstrating that in regions of greater BBBD, FW is also higher (Fig. 3). To test the association between BBBD echelon and the mean FW within each echelon, a MELR model was used that included a quadratic term for BBBD echelon. A likelihood ratio test confirmed a better fit for the quadratic term compared to a linear term ($p < 0.001$). Across all participants, greater BBBD was associated with greater mean FW with an R^2 of 0.47 for the full model ($p < 0.001$) (Table 2).

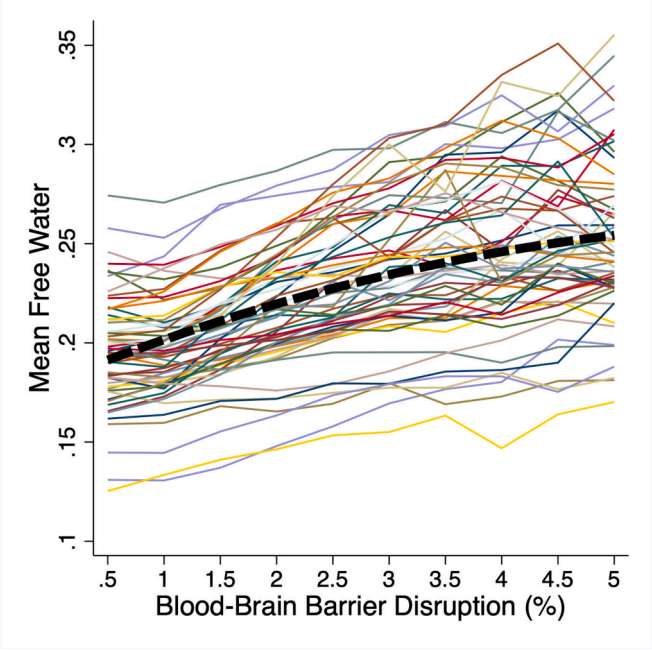

Fig. 3. Elevated free water (FW) colocalizes with increased blood–brain barrier disruption (BBBD). White matter was divided into echelons by the degree of BBBD from 0 to 5 % (interval 0.5 %). Mean FW within each BBBD echelon was calculated and FW vs BBBD echelon was plotted for each participant. Mixed effects linear regression and a quadratic term for BBBD demonstrated that increasing BBBD was associated with increasing FW ($p < 0.001$).

Table 2
Association between Blood-Brain Barrier Disruption and White Matter DTI Metrics.

Model with Linear BBBD term	**Beta Coefficient**		**R^2 for model**	***p-value***
Free Water	0.35 [0.33 to 0.37]		0.46	<0.001
FA corrected	0.34 [0.31 to 0.36]		0.40	<0.001
MD corrected	0.34 [0.31 to 0.37]		0.40	<0.001
Model with Quadratic BBBD term	**Beta, Linear Term**	**Beta, Quadratic Term**	**R^2 for model**	***p-value***
Free Water	0.57 [0.48 to 0.66]	−0.040 [-0.056 to −0.025]	0.47	<0.001*
FA corrected	0.73 [0.60 to 0.86]	−0.072 [-0.095 to −0.050]	0.41	<0.001*
MD corrected	0.41 [0.28 to 0.53]	−0.012 [-0.017 to 0.023]	0.40	0.28

Each DTI metric was converted to a Z-score to facilitate comparison across metrics. Separate mixed effects linear regression models were used to predict each mean DTI Z-score across all white matter. All models include covariates for age, sex, race, and MRI site. For each metric, a linear term and a quadratic term for BBBD were tested, and regression coefficients and [95 % confidence intervals] are shown. *Indicates better fit for quadratic over linear model using Wald test with $p < 0.001$. BBBD: Blood-brain Barrier Disruption; FA: fractional anisotropy; MD: mean diffusivity; CI: confidence interval; Std: Standardized.

3.5. Comparison of DTI Metrics

BBBD was used to predict each DTI metric after converting to a Z-score to compare metrics. Standardized coefficients and R^2 values are presented in Table 2. FW demonstrated the strongest association with BBBD with an R^2 of 0.47, compared to 0.41 for FAc, and 0.40 for MDc (Table 2). While the quadratic term for BBBD provided a better fit than a linear term for FW and FAc, the fit was numerically, but not significantly, greater for MDc.

3.6. Clinical Predictors of Free Water, Blood-Brain Barrier Disruption, or Cognitive Performance

Next, we tested whether clinical risk factors were associated mean

FW or BBBD across the entire white matter, or cognitive performance on the MoCA. In adjusted multivariable mixed regression models, older age (0.016 per decade; CI: 0.0098 to 0.023; $p < 0.001$) and more vascular risk factors (0.004 per risk factor, CI: 0.0011 to 0.0069; $p = 0.007$) were associated with higher mean white matter FW. Older age (0.0023 % per decade; CI: 0.0013 to 0.0034; $p < 0.001$) and Black race (0.0023 %; CI: 0.00012 to 0.0025; $p = 0.039$) were associated with greater BBBD in the WM. Older age (−1.07; CI: −1.95 to −0.20; $p = 0.017$), but not the number of vascular risk factors was associated with lower score on the MoCA test. In separate, unadjusted regressions, we did not find any associations between individual vascular risk factors (listed in Table 1) and mean white matter FW, BBBD, or MoCA score.

3.7. Comparison of Blood-Brain Barrier Disruption and Free Water Accumulation with Cognition

Finally, we tested whether FW or BBBD within each tissue region predicted performance on the MoCA. In unadjusted analyses, elevated FW was associated with lower MoCA score when measured in all WM (standardized Beta −0.42, CI: −0.66 to −0.19; $p < 0.001$), NAWM (std Beta −0.39; CI: −0.63 to −0.16; $p = 0.001$), penumbra (std Beta −0.34; CI: −0.58 to −0.10; $p = 0.005$; Fig. 4A), or WMH (std Beta −0.32; CI: −0.57 to −0.08; $p = 0.009$). More severe BBBD was associated with lower MoCA score when measured in all WM (std Beta −0.29; CI: −0.54 to −0.048; $p = 0.019$), NAWM (Std Beta −0.30; CI: −0.54 to −0.050; $p = 0.019$), and the penumbra (std Beta −0.32; CI: −0.56 to −0.077; $p = 0.010$; Fig. 4B), but not in WMH (std Beta −0.16; CI: −0.41 to 0.095; $p = 0.22$; Supplemental Table). The strongest association was in the penumbra, where higher FW (std Beta −0.36; CI: −0.62 to −0.11; $p = 0.005$) and more severe BBBD (std Beta −0.30; CI: −0.56 to −0.033; $p = 0.028$) were each independently associated with worse MoCA score while adjusting for age, sex, race, education, and study site as a random effect (Table 3). The raw regression coefficients are included in Table 3, but to provide context on the effect size, an increase in mean penumbra FW of 0.033, or an increase in mean penumbra BBBD of 0.004 % was associated with a 1-point lower MoCA score. Similar associations were seen across all white matter (FW: std Beta −0.50; CI: −0.77 to −0.23; $p < 0.001$; BBBD: std Beta −0.26; CI: −0.51 to −0.0081; $p = 0.043$) and in NAWM (FW: std Beta −0.41; CI: −0.64 to −0.19; $p < 0.001$; BBBD std Beta −0.24; CI: −0.46 to −0.021; $p = 0.032$), where higher FW and higher BBBD were independently associated with lower MoCA score in adjusted models.

Table 3
Multivariable Mixed-effects Regression Model to Predict MoCA Score (N = 58).

Predictor	Coefficient	95 % CI	Std Beta	Added R^2	P
Free Water in WMH Penumbra	−29.81	−50.47 to −9.15	−0.36	0.10	0.005
BBBD in WMH Penumbra	−232.07	−438.75 to −25.38	−0.30	0.062	0.028
Black Race	−1.38	−3.06 to 0.31	−0.21	0.033	0.11
Age (per decade)	−0.026	−1.06 to 1.00	−0.008	0	0.96
Education	−0.015	−0.23 to 0.21	−0.016	0.003	0.89
Female Sex	0.48	−1.05 to 2.01	0.078	0.005	0.54

Includes random effect for MRI site. For the full model: $R^2 = 0.26$, $p = 0.020$. MoCA = Montreal Cognitive Assessment, CI = confidence intervals, Std Beta = Standardized Beta, WMH = white matter hyperintensity, BBBD = blood–brain barrier disruption.

4. Discussion

In this sample of participants with a history of stroke or TIA at risk for VCID, more severe BBBD and greater FW accumulation were each independently associated with worse cognitive performance. Additionally, we confirmed that in regions with more severe BBBD, there were greater levels of FW accumulation. These findings support the hypothesized mechanism for the pathogenesis of WMH in which disruption of the BBB in the NAWM allows solutes and proinflammatory molecules to enter the interstitium leading to increased FW (Wardlaw et al., 2019; Alber et al., 2019; Rosenberg, 2022). To our knowledge, this is the first report detailing this relationship between BBBD measured using DSC and DTI free water in humans.

In addition to providing insight into the pathogenesis of CSVD in participants with prior ischemic stroke, this study also provides validation for two imaging biomarkers of CSVD pathology that were sensitive to cognitive differences: DTI-based FW and DSC-based BBB permeability. DTI is an established biomarker for microstructural integrity, however its use in measuring FW has been in dispute particularly in the absence of multi-shell diffusion imaging (Golub et al., 2021). Similarly, the use of DSC imaging to measure BBBD has been

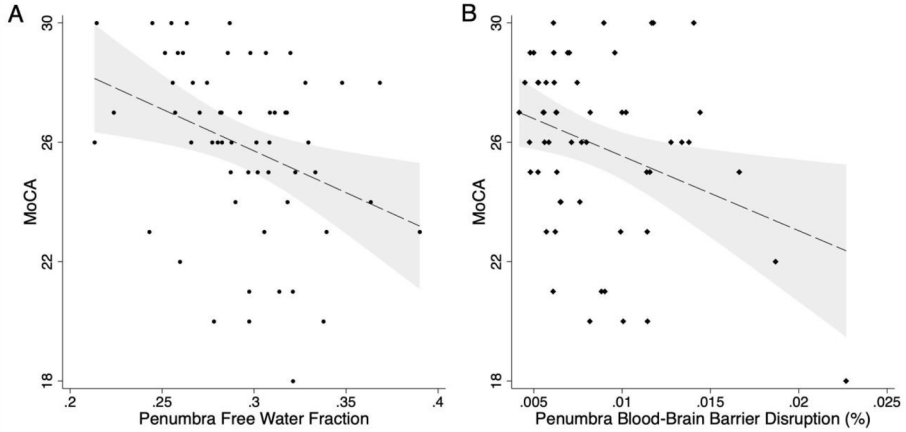

Fig. 4. Free water and blood–brain barrier disruption (BBBD) are associated with cognitive performance. A) Higher mean free water in the white matter hyperintensity (WMH) penumbra (standardized Beta = -0.34; $p = 0.008$) was associated with worse performance on the Montreal Cognitive Assessment (MoCA). B) Greater BBBD in the WMH penumbra (std Beta = -0.32, $p = 0.014$) was also associated with lower MoCA score. Dashed line shows predicted MoCA score derived from a multivariable linear regression model, in which both mean FW (std Beta = -0.36, $p = 0.005$) and mean BBBD (std Beta = -0.30, $p = 0.028$) in the WMH penumbra were independently associated with MoCA score while covarying for age, sex, race, education, and MRI site as a random effect. Gray area reflects 95 % confidence intervals.

called into question when applied to CSVD (Thrippleton et al., 2019). However, in our study, these two biomarkers, which are derived from very different magnetic resonance principles, were aligned as biomarkers of CSVD pathology. Of note, a prior study using a different measure of BBBD (Dynamic contrast enhanced MRI) and a different measure of tissue diffusivity (intravoxel incoherent motion DTI) also found associations between the two measures in the perilesional white matter in patients with CSVD. They used a longitudinal design and demonstrated that BBBD was associated with change in parenchymal diffusivity 2 years later (Kerkhofs et al., 2021). Furthermore, another recently published, complementary study also found an association between whole-brain BBB dysfunction, measured via diffusion-prepared arterial spin labelling (DP-ASL) water exchange, and white matter FW in older volunteers without dementia or stroke (Pappas et al., 2024). In that study, lower BBB water exchange and higher FW were also associated with executive function, with higher FW mediating the association between BBB dysfunction and cognitive performance. Taken together, these studies support the hypothesis that BBB dysfunction contributes to the pathogenesis of cognitive impairment in CSVD and vascular aging.

The sample in this study consisted of participants who presented with a stroke, typically minor stroke given the disability-based exclusions, and were found to have CSVD in the form of WMH on their MRI. This is a very common scenario and represents a cohort of patients thought to be at high risk for VCID (Rost et al., 2022). Current management for this population is focused on secondary stroke prevention and risk factor control. Despite this, in this study, where participants were scanned at least 3 months after their event, we found that these two biomarkers, which most likely reflect an inflammatory process, were proportional to cognitive performance. While aspirin and statins do have anti-inflammatory effects, these findings suggest that direct targeting of the inflammatory response should be investigated further as a potential treatment for post-stroke cognitive impairment.

Our finding that white matter regions with higher BBBD colocalized with higher mean FW was very robust. As depicted in the spaghetti plot in Fig. 3, every participant showed this positive association. This relationship was best fit with a quadratic term for BBBD, indicating that the association was strongest in the intermediate ranges of BBBD compared to the regions of highest BBBD. This finding may be explained by a saturation effect of accumulating FW in white matter tissue. While DTI metrics are often highly collinear since they are derived from the same acquisition, we found that the association between BBBD and FW was strongest compared to the associations with FAc or MDc, suggesting a relative specificity for the FW measure. In this analysis, FAc was positively associated with BBBD, which is counterintuitive since low FA is typically associated with white matter injury. This finding is best explained by the anatomical gradient of FA, where FA is lower in peripheral structures and highest in central white matter structures where WMH occur and more BBBD is seen.

The strengths of our study include standardized data collected from two centers, the utilization of two different types of imaging biomarkers, and imaging performed during the chronic phase after stroke. The primary limitation of this study is the lack of a gold standard to validate the biomarkers. However, it is notable that higher BBBD colocalized with higher mean FW in every participant. In the absence of pathology samples, which are typically not available in human studies of stroke and cognition, this may be as close as we can get to ground truth. Another limitation is the resolution at which the DTI and DSC were acquired. The anisotropic voxels of the DTI sequence (1.7x1.7x2.5 mm) might impact the calculation of DTI metrics and introduce bias depending on head position and fiber orientation. However, averaging over larger ROIs may mitigate this bias. Likewise, the DSC acquisition (2.3x2.3x7mm) is the limiting resolution, but is better than non-contrast ASL sequences for localizing BBB dysfunction and is shorter duration. BBBD is calculated from the source images of a DSC-PWI acquisition, a sequence which is clinically available on modern MRI scanners and used in acute stroke MRI protocols. Also, two different formulations of gadolinium contrast were used in the study which may have affected the BBB analysis. Additional limitations include a modest sample size, the cross-sectional design, and the use of a brief cognitive screening test rather than more extensive neuropsychological testing. Additionally, since patients in the study had a history of stroke, it is not known how the stroke itself may have affected cognition, separate from the effects of CSVD. Longitudinal studies using these biomarkers should test whether BBBD precedes FW accumulation and cognitive decline. Finally, the participants in this study had a high level of education (100 % completed high school, 50 % had a graduate degree), impacting the generalizability of the study. Higher education is associated with better cognitive performance, possibly through increased cognitive reserve, and can lead to a ceiling effect on the MoCA.

5. Conclusions

In participants at risk for VCID due to a history of stroke and the presence of CSVD, we observed disruption of the blood–brain barrier and the concomitant accumulation of FW, both of which were associated with cognitive performance. These biomarkers represent a potential target for further treatments to prevent VCID.

CRediT authorship contribution statement

Kyle C. Kern: Writing – review & editing, Writing – original draft, Validation, Formal analysis, Data curation, Conceptualization. **Marwah S. Zagzoug:** Writing – review & editing, Project administration, Data curation. **Rebecca F. Gottesman:** Writing – review & editing, Supervision, Methodology, Funding acquisition. **Clinton B. Wright:** Writing – review & editing, Supervision, Methodology, Conceptualization. **Richard Leigh:** Writing – review & editing, Supervision, Project administration, Methodology, Investigation, Funding acquisition, Formal analysis, Data curation, Conceptualization.

Declaration of competing interest

The authors declare that they have no known competing financial interests or personal relationships that could have appeared to influence the work reported in this paper.

Acknowledgements

The authors thank the research teams and clinical Stroke teams at the National Institute of Neurological Disorders and Stroke (NINDS) Intramural Stroke Branch, Suburban Hospital and Medstar Washington Hospital Center. This work utilized the resources of the NIH Biowulf high performance computing cluster (hpc.nih.gov). The authors thank Ying Kuen Cheung, PhD for advice on statistical analysis.

6. *Sources of Funding*

This study was supported by the NINDS intramural research program at NIH.

R.L. is supported by NIH grant R01NS123386.

Disclosures.

CBW reports honoraria from Uptodate.com for articles written on vascular dementia. The other authors report no disclosures.

Author Contributions

Kyle C. Kern: Drafted the article, made a substantial contribution to the acquisition of data and analysis and interpretation of data, revised the article critically for important intellectual content and approved the version to be published.

Marwah S. Zagzoug: Made a substantial contribution to the concept

and design, acquisition of data or analysis and interpretation of data, revised the article critically for important intellectual content and approved the version to be published.

Rebecca F. Gottesman: Made a substantial contribution to the analysis and interpretation of data, revised the article critically for important intellectual content and approved the version to be published.

Clinton B. Wright: Made a substantial contribution to the concept and design, substantial contribution to the analysis and interpretation of data, revised the article critically for important intellectual content and approved the version to be published.

Richard Leigh: Made a substantial contribution to the concept and design, substantial contribution to the analysis and interpretation of data, revised the article critically for important intellectual content and approved the version to be published.

Appendix A. Supplementary data

Supplementary data to this article can be found online at https://doi.org/10.1016/j.nicl.2024.103706.

Data availability

Data will be made available on request.

References

Adams Jr., H.P., Bendixen, B.H., Kappelle, L.J., Biller, J., Love, B.B., Gordon, D.L., Marsh, E.E., 1993. 3rd. Classification of subtype of acute ischemic stroke. Definitions for use in a multicenter clinical trial. TOAST. Trial of Org 10172 in Acute Stroke Treatment. Stroke. 24, 35–41. https://doi.org/10.1161/01.str.24.1.35.

Alber, J., Alladi, S., Bae, H.J., Barton, D.A., Beckett, L.A., Bell, J.M., Berman, S.E., Biessels, G.J., Black, S.E., Bos, I., et al., 2019. White matter hyperintensities in vascular contributions to cognitive impairment and dementia (VCID): Knowledge gaps and opportunities. Alzheimers Dement (n y). 5, 107–117. https://doi.org/10.1016/j.trci.2019.02.001.

Bani-Sadr, A., Mechtouff, L., De Bourguignon, C., Mauffrey, A., Boutelier, T., Cho, T.H., Cappucci, M., Ameli, R., Hermier, M., Derex, L., et al., 2023. Blood-Brain Barrier Permeability and Kinetics of Inflammatory Markers in Acute Stroke Patients Treated With Thrombectomy. Neurology. 101, e502–e511. https://doi.org/10.1212/WNL.0000000000207460.

Boxerman, J.L., Schmainda, K.M., Weisskoff, R.M., 2006. Relative cerebral blood volume maps corrected for contrast agent extravasation significantly correlate with glioma tumor grade, whereas uncorrected maps do not. AJNR AmJNeuroradiol. 27, 859–867, 27/4/859 [pii].

Cerri, S., Puonti, O., Meier, D.S., Wuerfel, J., Mühlau, M., Siebner, H.R., Van Leemput, K., 2021. A contrast-adaptive method for simultaneous whole-brain and lesion segmentation in multiple sclerosis. Neuroimage. 225, 117471. https://doi.org/10.1016/j.neuroimage.2020.117471.

Debette, S., Markus, H.S., 2010. The clinical importance of white matter hyperintensities on brain magnetic resonance imaging: systematic review and meta-analysis. BMJ. 341, c3666. https://doi.org/10.1136/bmj.c3666.

Fazekas, F., van Buchem, M., Mok, V., DeCarli, C., Werring, D., Viswanathan, A., Barkhof, F., Biessels, G.J., Black, S.E., Brayne, C., et al., 2013. Neuroimaging standards for research into small vessel disease and its contribution to ageing and neurodegeneration. The Lancet Neurology. 12, 822–838. https://doi.org/10.1016/s1474-4422(13)70124-8.

Golub, M., Neto Henriques, R., Gouveia, N.R., 2021. Free-water DTI estimates from single b-value data might seem plausible but must be interpreted with care. Magn Reson Med. 85, 2537–2551. https://doi.org/10.1002/mrm.28599.

Jin, S., Han, S., Stoyanova, R., Ackerstaff, E., Cho, H., 2019. Pattern recognition analysis of dynamic susceptibility contrast (DSC)-MRI curves automatically segments tissue areas with intact blood-brain barrier in a rat stroke model: A feasibility and comparison study. J Magn Reson Imaging. https://doi.org/10.1002/jmri.26949.

Kerkhofs, D., Wong, S.M., Zhang, E., Staals, J., Jansen, J.F.A., van Oostenbrugge, R.J., Backes, W.H., 2021. Baseline Blood-Brain Barrier Leakage and Longitudinal Microstructural Tissue Damage in the Periphery of White Matter Hyperintensities. Neurology. 96, e2192–e2200. https://doi.org/10.1212/WNL.0000000000011783.

Kern, K.C., Zagzoug, M.S., Gottesman, R.F., Wright, C.B., Leigh, R., 2023. Diffusion Tensor Free Water MRI Predicts Progression of FLAIR White Matter Hyperintensities After Ischemic Stroke. Frontiers in Neurology. 14, 1172031. https://doi.org/10.3389/fneur.2023.1172031.

Kloppenborg, R.P., Nederkoorn, P.J., Geerlings, MIa., 2014. Presence and progression of white matter hyperintensities and cognition: A meta-analysis. Neurology. https://doi.org/10.1212/WNL.0000000000000505.

Leigh, R., Jen, S.S., Varma, D.D., Hillis, A.E., Barker, P.B., 2012. Arrival Time Correction for Dynamic Susceptibility Contrast MR Permeability Imaging in Stroke Patients. PLoSOne. 7, e52656.

Maillard, P., Fletcher, E., Harvey, D., Carmichael, O., Reed, B., Mungas, D., DeCarli, C., 2011. White matter hyperintensity penumbra. Stroke. 42, 1917–1922. https://doi.org/10.1161/STROKEAHA.110.609768.

Mayer, C., Nagele, F.L., Petersen, M., Frey, B.M., Hanning, U., Pasternak, O., Petersen, E., Gerloff, C., Thomalla, G., Cheng, B., 2022. Free-water diffusion MRI detects structural alterations surrounding white matter hyperintensities in the early stage of cerebral small vessel disease. J Cereb Blood Flow Metab. 271678X221093579. https://doi.org/10.1177/0271678X221093579.

Pappas, C., Bauer, C.E., Zachariou, V., Maillard, P., Caprihan, A., Shao, X., Wang, D.J.J., Gold, B.T., 2024. MRI free water mediates the association between water exchange rate across the blood brain barrier and executive function among older adults. Imaging Neurosci (camb). 2, 1–15. https://doi.org/10.1162/imag_a_00183.

Promjunyakul, N., Lahna, D., Kaye, J.A., Dodge, H.H., Erten-Lyons, D., Rooney, W.D., Silbert, L.C., 2015. Characterizing the white matter hyperintensity penumbra with cerebral blood flow measures. Neuroimage Clin. 8, 224–229. https://doi.org/10.1016/j.nicl.2015.04.012.

Rosenberg, G.A., 2022. Willis Lecture: Biomarkers for Inflammatory White Matter Injury in Binswanger Disease Provide Pathways to Precision Medicine. Stroke. 53, 3514–3523. https://doi.org/10.1161/STROKEAHA.122.039211.

Rosenberg, G.A., Wallin, A., Wardlaw, J.M., Markus, H.S., Montaner, J., Wolfson, L., Iadecola, C., Zlokovic, B.V., Joutel, A., Dichgans, M., 2016. Consensus statement for diagnosis of subcortical small vessel disease. Journal of Cerebral Blood Flow & Metabolism. 36, 6–25.

Rost, N.S., Cougo, P., Lorenzano, S., Li, H., Cloonan, L., Bouts, M.J., Lauer, A., Etherton, M.R., Karadeli, H.H., Musolino, P.L., et al., 2018. Diffuse microvascular dysfunction and loss of white matter integrity predict poor outcomes in patients with acute ischemic stroke. J Cereb Blood Flow Metab. 38, 75–86. https://doi.org/10.1177/0271678X17706449.

Rost, N.S., Brodtmann, A., Pase, M.P., van Veluw, S.J., Biffi, A., Duering, M., Hinman, J. D., Dichgans, M., 2022. Post-Stroke Cognitive Impairment and Dementia. Circ Res. 130, 1252–1271. https://doi.org/10.1161/CIRCRESAHA.122.319951.

Savva, G.M., Stephan, B.C., 2010. Alzheimer's Society Vascular Dementia Systematic Review G. Epidemiological studies of the effect of stroke on incident dementia: a systematic review. Stroke. 41, e41–e46. https://doi.org/10.1161/STROKEAHA.109.559880.

Thrippleton, M.J., Backes, W.H., Sourbron, S., Ingrisch, M., van Osch, M.J.P., Dichgans, M., Fazekas, F., Ropele, S., Frayne, R., van Oostenbrugge, R.J., et al., 2019. Quantifying blood-brain barrier leakage in small vessel disease: Review and consensus recommendations. Alzheimers Dement. 15, 840–858. https://doi.org/10.1016/j.jalz.2019.01.013.

Wardlaw, J.M., Smith, C., Dichgans, M., 2019. Small vessel disease: mechanisms and clinical implications. Lancet Neurol. 18, 684–696. https://doi.org/10.1016/S1474-4422(19)30079-1.

Zaharchuk, G., 2007. Theoretical basis of hemodynamic MR imaging techniques to measure cerebral blood volume, cerebral blood flow, and permeability. AJNR AmJNeuroradiol. 28, 1850–1858, 28/10/1850 [pii];10.3174/ajnr.A0831 [doi].